Hmmier and Dowling
Future Journal of Pharmaceutical Sciences (2024) 10:133
https://doi.org/10.1186/s43094-024-00712-3

Future Journal of Pharmaceutical Sciences

RESEARCH Open Access

In vitro evaluation of the clinical utility of Apitolisib/Vorinostat combination in Apitolisib-resistant H1975 lung adenocarcinoma cells

Abduladim Hmmier[1*] and Paul Dowling[2]

Abstract

Background The PI3K signalling pathway regulates the metabolic activity of cells. Disruption by PI3K inhibitors causes an aerobic/anaerobic imbalance that decreases energy production and cell growth. Cancer cells adapt to PI3K inhibitors in order to reduce their effectiveness. Resistance to Apitolisib could be due to intrinsic factors or acquired adaptation. Oncologists often ask whether to discontinue Apitolisib, increase its dose, or use a drug combination.

Methods We observed the proliferation of resistant cells in (H1975R+) and out (H1975R–) of Apitolisib treatment, cell cycle pattern, energy phenotyping/reprogramming, and the effects of combining Apitolisib with Vorinostat on the acquired proliferation of H1975R– cells.

Results The Proliferation of H1975R– cells increased, while that of H1975R+ cells remained suppressed. Both conditions showed a 5 × decrease in the number of cells at the Go/G1 phase and doubled at S and G2/M phases ($p < 0.0001$). Both H1975R– and H1975R+ cells exhibited decreased ECAR, with a stronger effect observed in H1975R+ cells ($p < 0.0001$). Oxygen consumption (OCR) increased significantly in H1975R– compared with that in H1975P ($p = 0.02$). The resistant cells became energetically active using mitochondrial respiration in drug-free medium; H1975R+ was hypo-energetic and consumed more free fatty acids ($p = 0.0001$). Ketone bodies in H1975R+ were increased by 40% and 2 × in BOHB and AcAc levels, respectively, compared to that in H1975P and H1975R– ($p < 0.0001$). H1975R– cell survival was 80% compared with 20% in H975R+ cells treated with 7 µM Vorinostat. Vorinostat effectively controlled acquired hyperproliferation of H1975R– cells.

Conclusion If a tumour becomes unresponsive to Apitolisib, it is advisable to continue the inhibitor and consider a combination with non-tyrosine kinase inhibitors.

Keywords H1975 lung adenocarcinoma, Apitolisib-acquired resistance, Acquired aggressive proliferation, Metabolic reprogramming, Apitolisib/Vorinostat combination

Background

The primary aim of chemotherapy is to disrupt the proliferation and dissemination of malignant tumours as well as to facilitate the process of programmed cell death known as apoptosis. These are accomplished by the deactivation of molecular machinery implicated in the cell cycle, cell viability, and energy generation, all of which rely on the activation of signalling pathways known as

*Correspondence:
Abduladim Hmmier
hmmier@icloud.com
[1] Clinical Proteomics Research Group, Libyan Biotechnology Research Centre, Tripoli, Libya
[2] Biology department, Clinical Proteomics Lab., Maynooth University, Maynooth, Ireland

protein tyrosine kinase (PTK) cascades [1]. Protein tyrosine kinases (PTKs) are meant to phosphorylate tyrosine-residue-containing enzymes utilizing ATP. Based on their location, PTKs are classified into receptor tyrosine kinases (RTKs), located in the cell membrane, such as vascular endothelial growth factor receptor (VEGFR), growth factors receptor (GFR), Insulin receptor (IR), colony-stimulating factor 1 receptor (CSF1R), hepatocyte growth factor receptor (HGFR) and Fibroblast growth factor receptor (FGFR), and non-receptor tyrosine kinases (NRTKs), located in the cytoplasm, like Janus kinase (JAK), focal adhesion kinase (Fak), and proto-Oncogenes; such as Abl, FES and Scr, their function is to regulate cell proliferation, migration, adhesion, apoptosis and immuno-modulation through coupling with the RTKs and other G-coupled receptors [2]. Consequently, clinical trials have introduced tyrosine kinase inhibitors (TKI), which specifically target both RTK and NRTK. Over the past two decades, some of these inhibitors have been approved by the FDA, contributing to the enhancement of patient survival and quality of life [3]. The selection of the appropriate RTK or a cytoplasmic NRTK depends on the presence of a "gain of function" mutation in the specific TK such as R1275Q in the anaplastic lymphoma receptor (ALK) and F1147L mutation in neuroblastoma (NB) gene and/or its abundance within the cell leading to activation of the downstream signalling pathways [4]. Despite the effective treatment of solid tumours with targeted chemotherapy, the remarkable capacity of tumour cells to develop resistance to these inhibitors has been frustrating. Acquired resistance to tyrosine kinase inhibitors is characterized by the re-establishment of phosphorylation of pivotal proteins, potentially facilitated through crosstalk with other upstream or downstream tyrosine kinases such as pim kinase, Janus kinase (JAK), mitogen-activated protein kinase (MAPK), and hepatocyte growth factor receptor (HGFR) [5]. Yang, Y. et al. in 2022 wrote an outstanding review detailing protein tyrosine kinases, their activation associated mutations, their small molecule inhibitors, and the possible molecular mechanisms of resistance to such TKIs [5]. The overall result is the restoration of the tumour cell phenotype, leading to the acquisition of more aggressive metabolic reprogramming [6]. However, to understand the mechanism underlying metabolic reprogramming during tumorigenesis and tyrosine kinase treatment/resistance, the subject of this manuscript, it is imperative to consider cancer cells as somatic cells that have undergone specific mutations (known as driver mutations), causing them to exhibit distinct behaviours compared to normal cells. Consequently, they undergo glucose metabolic reprogramming, switching to glycolysis, to meet the increased requirements for nucleic acid synthesis. If glucose metabolism remained the same as in normal somatic cells, the influx of glucose would be insufficient to satisfy the demand for nucleic acid synthesis needed by the highly proliferative immortalized cells. As a result, a portion of this metabolic reprogramming involves the cessation of complete mitochondrial oxidation of glucose and the activation of fatty acid and amino acid utilization instead [7, 8]. The PI3K pathway plays a significant role in metabolic reprogramming by enhancing glucose uptake and utilization [9]. Moreover, the m-TOR signalling pathway enables the activation of amino acid utilization as an alternative source of energy production in the mitochondria [10]. The PI3K/mTOR pathway plays a crucial role in cell cycle progression, proliferation, and the prevention of apoptosis [11]. The activation of this pathway has been observed in various solid tumours. Clinical trials of PI3K/mTOR inhibitors have been conducted, although the resistance of tumour cells to such chemotherapy has been well documented [12].

The question consistently posed by oncologists when tumour cells cease responding or when tumour relapse is encountered is, what course of action should be taken? Should Apitolisib be discontinued? Should the Apitolisib dosage be increased? Should further analysis be conducted to identify any possible novel passenger mutations that could affect the activity of the PI3K/mTOR signalling pathway? Or should the consideration of additional drug combinations be entertained? To address these questions, resistance to Apitolisib was induced by subjecting H1975 lung adenocarcinoma cells to a training process of continuous exposure to increasing doses of Apitolisib. The resistant H1975 cells, both in (H1975R+) and out (H1975R−) of the drug incubation, were then compared to their Apitolisib-naïve sensitive counterparts (H1975P). To understand the resistance to Apitolisib from a metabolic reprogramming perspective, we observed their proliferation rate, which signifies the quantity of energy generated. Next, we analysed their cell cycle and energy phenotyping using Cytel® cell cycle profiling, Seahorse®, and a central carbon metabolism assay kit, respectively. Based on these results, an additional experiment was performed to impede the progressive proliferation of resistant cells using a pan-histone deacetylase inhibitor (Vorinostat). The purpose of this study was not to explore the molecular basis of resistance to Apitolisib but rather to examine a clinical approach to managing this resistance.

Materials and methods

Apitolisib-resistant H1975 cells were developed by the thoracic oncology research group, Trinity Translational Medicine Institute (TTMI) at Saint James's Hospital, and kindly gifted to us by the group leader Dr. Kathy Gately.

Cell culture: Apitolisib-naïve parent (P) and resistant (R) H1975 lung adenocarcinoma cells were cultured in RPMI-1640 medium (Sigma R5886 Lot: RNBF1079) supplemented with 10% (FBS Sigma, F7524, Lot: BCBR 1178V) and 1% penicillin-streptomycin-glutamine (Gibco Cat No: 10378-016). The media for H1975R cells were conditioned with 1 μM Apitolisib (H1975R+) or Apitolisib-free media (H1975R−).

Confluency test: H1975P, H1975R+ and H1975R− cells were passaged in, vented and tilted neck, T75 flasks. The proliferation of these cells was observed until 90% confluency was achieved.

Growth curve: T75 flasks, at 75% confluency, of H1975P and H1975R cells (in/out of drug incubation) were sub-cultured in five T75 flasks. The cells were left to adhere for 24 h. RPMI was then changed daily. One flask was removed per condition each day, trypsinized, and the turbidity of the cell suspension in PBS was measured as the OD at 600 nm. Growth curves were plotted as optical density versus time.

Cell cycle profiling: Cells were seeded in sterile Nunc™ MicroWell™ 96-well microplates in six replicates: H1975P, H1975R− and H1975R+. Cells were allowed to adhere and proliferate for 48 h, washed twice with 1× PBS, fixed in pre-warmed (37 °C) formaldehyde (Image-iT™ Fixative Solution; 4% formaldehyde, methanol free, Cat #FB002) containing 0.3% Triton-X100 for 15 min at 37 °C. The cells were then washed twice with 1× PBS and the nuclei were stained with DAPI (Invitrogen™-DAPI, cat. #D3571) for 15 min at RT. The cell cycle was read in a Cytel® Cell Imaging System (GE Healthcare Life Sciences).

Metabolic profiling: A Seahorse XF24 extracellular flux analyser and Seahorse XF24 FluxPak mini kit (Part #100,867-100) were used. A preliminary experiment was conducted to determine the optimal seeding density. Cells were seeded in 24-well cell culture plates (Seahorse Bioscience V7-PS, TC-treated, Part #100,777-004) at densities of 60,000, 40,000, and 80,000 cells/well for H1975P, H1975R−, and H1975R+, respectively [13]. The results from the Seahorse XF24 analyser were normalized by dividing their values by their corresponding crystal violet measurements [13]. The average of six OCR, PPP, and ECAR per condition was recorded. The experiment was performed once a week for three consecutives. Normalized OCR, PPP, and ECAR values were compared using GraphPad Prism® 7.0. The Seahorse XF energy phenotype test report from Agilent® was used to track the metabolic changes in the compared cells.

Central carbon metabolism: This was evaluated using the colorimetric Enzychrom™ pyruvate assay kit (Cat #EPYR-100), free fatty acid assay kit (Cat #EFFA-100), and EnzyChrom™ ketone assay kit (EKBD-100) in accordance with the guidelines provided by the manufacturer.

Drug combination: Vorinostat (Sigma-Aldrich, CAS. #149,647-78-9) was used as a pan-histone deacetylase (HDAC) inhibitor. BrdU cell proliferation colorimetric ELISA assay kit, purchased from Cell Signalling Technology® (cat. no. 6813), was used to construct a dose–response curve for cell proliferation. The Vorinostat dose ranged used was from 1 to 20 μM (represented as log 3–log 4.3 in the graph). The log-dose response versus the % inhibition of growth was constructed in Prism 7.0.

Results

Confluency test: H1975P cells became 90% confluent within three days, whereas the H1975R− cells took only two. Furthermore, H1975R+ cells required five days to reach 90% confluency.

Proliferation rates: Fig. 1 illustrates a qualitative comparison of the proliferation rate of H1975R cells with that of H1975P cells. Evidently, H1975R− developed adaptive mechanisms, allowing them to proliferate more rapidly than H1975P cells. Additionally, a significant decline in the proliferation rate of H1975GR+ was observed. The slow proliferation of H1975GR+ cells is indicative of a pure metabolic reprogramming/bypass of the PI3K/mTOR pathway. In contrast, the aggressive proliferation of H1975R− cells was the sum of the advantageous metabolic reprogramming and the restoration of PI3K/mTOR signalling.

Cell cycle profiling: Fig. 2 depicts the cell cycle pattern for H1975 cells. In the reference cell cycle pattern

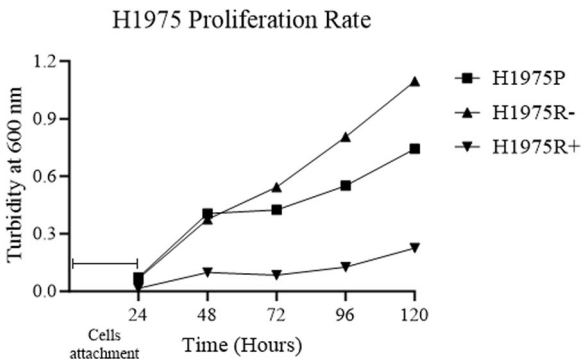

Fig. 1 Growth curves of H1975P (Apitolisib naive/sensitive) and H1975R (Apitolisib resistant) cells, in the presence (H1975R+) or absence (H1975R–) of Apitolisib incubation. The y-axis represents the five OD points, which correspond to consecutive five-day measurements of detached cells suspension in 1 × PBS. The x-axis, on the other hand, represents the time interval in hours between these measurements. The comparison between the tested cells only commenced after 48 h, as Apitolisib was added to the treated H1975R+ after the initial 24 h (zero-time), allowing for proper cells adherence and resuscitation

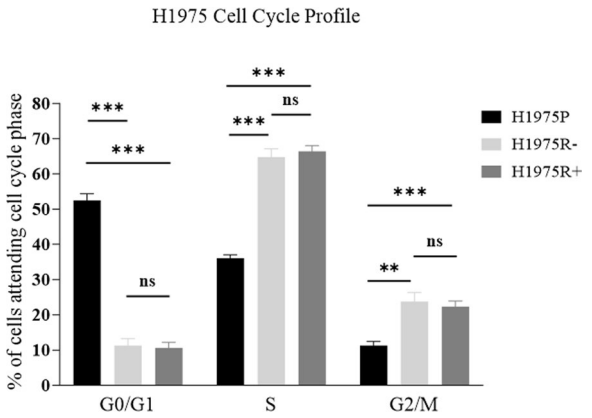

Fig. 2 Cytel® cell cycle profiling of H1975 lung adenocarcinoma cells. The Apitolisib-sensitive H1975 cells (H1975P: n = 14,504 ± 1852) were compared to the Apitolisib resistant H1975 cells that were incubated in 1 µM Apitolisib during the entire experiment (H1975R+: n = 3793 ± 525). Additionally, the Apitolisib-resistant H1975 cells were grown in drug-free medium for a total of five passages (two weeks), including the experiment (H1975R−: n = 12,167 ± 911). It is important to note that the H1975R+ cells were continuously maintained in the presence of 1 µM Apitolisib all the time, both before and during the experiment. The different phases of the cell cycle are represented as follows: G0 for newly divided cells, G for the growth phase/cell maturation, S for the synthesis phase, G2 is a second maturation phase prior to cell division, and M for the mitosis phase. The statistical analysis revealed significant differences between the groups, with a *p* value of 0.0–0.5 (ns), 0.00001 (**) for some comparisons and < 0.000001 (***) for others

(H1975P), the percentage of cells attending G0/G1 was 52% of the total cell number, which was approximately the sum of cells attending S and G2/M. The percentage of cells in the S phase was triple (36%) the number of cells in the G2/M phase. Both H1975R+ and H1975R- exhibited a doubling of the percentage of cells in the S and G2/M phases compared to H1975P cells ($p < 0.0001$). Additionally, the percentage of cells in the G0/G1 phase was five times lower in both H1975R− and H1975R+ than in H1975P cells ($p < 0.0001$). Notably, no difference in the cell cycle pattern was observed between H1975R− and H1975R+ cells. Specifically, the cells in the G0/G1 phases accounted for 11.3% and 10.6%, respectively, the cells in the S phase accounted for 64.7% and 66.4%, respectively, and the cells in the G2/M phases accounted for 23.8% and 22.4%, respectively. Furthermore, it should be noted that the changes observed in H1975R+ cells were permanent, as evidenced by their retention even after treatment withdrawal for five passages (15 days).

Energy phenotyping: Fig. 3 shows the variations in the ECAR/PPR/OCR parameters between H1975R+, H1975R− cells, and their parent Apitolisib-sensitive cells (H1975P). Additionally, the figure shows the effect of 1 µM Apitolisib on the energy phenotype of Apitolisib-resistant H1975 cells. ECAR was significantly reduced in both H1975R− and treated H1975R+ cells ($p < 0.0001$). However, this effect was more pronounced in H1975R+ cells. The H1975R− cells exhibited a significant increase in the OCR, as indicated by a decrease in the oxygen concentration in the assay medium relative to H1975P cells ($p = 0.02$). This increase in oxygen

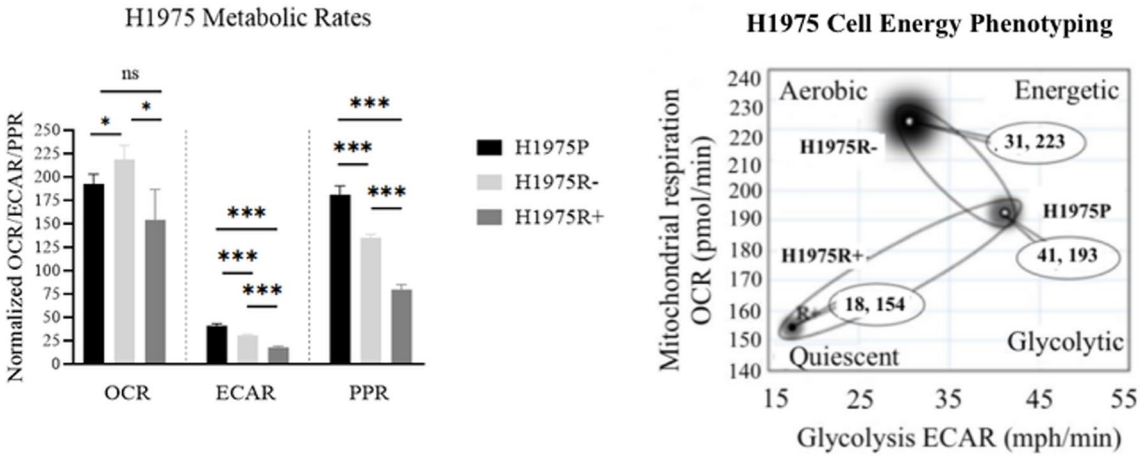

Fig. 3 Seahorse energy phenotyping of Apitolisib-resistant H1975 cells in the presence (R+) or absence (R−) of Apitolisib compared to their Apitolisib-naive sensitive cells. Aerobic phenotype demonstrates the mitochondrial respiration activity measured by the ability of the cells to consume oxygen (OCR measured as pmol/min), while the glycolytic phenotype indicates active Warburg effect on glucose metabolism as measured by the extracellular acidification rate (ECAR measured as mpH/min). PPR is the total of protons produced from both glycolytic and mitochondrial respiration sources (PPRtot = PPRglyc + PPRresp and can also be calculated by dividing the $ECAR_{tot}$ by the buffering power measured as pmolH+ /min/µg protein). Quiescent phenotype indicates very weakly energetic cells. Energetic phenotype indicates highly energetic cells. (ns): $p = 0.6$, (*): $p = 0.01–0.02$, (***): $p < 0.0001$

consumption was mitigated by incubation with Apitolisib. Additionally, mitochondrial oxidative respiration (OCR) was significantly reduced in the H1975R+cells compared to that in the H1975R− cells ($p=0.01$). Through cell energy phenotyping, it was observed that the H1975R− cells possessed greater energy levels than the H1975P cells, and they appeared to favour mitochondrial oxidative respiration, potentially through the aerobic utilization of glucose and other acetyl-CoA precursors, rather than relying on glycolysis. In summary, based on the phenotypic characterization of cellular energy, it was observed that H1975R− cells demonstrated heightened levels of energy when compared to the H1975P cells. The former exhibited a preference for aerobic metabolism. Following exposure to 1 μM Apitolisib, resistant cells (H1975R+) tended to enter a quiescent or hypo-energetic state, leading to a decline in both glycolysis and mitochondrial respiration due to the inhibition of PI3K-AKT/m-TOR phosphorylation.

Central carbon metabolism: Fig. 4 illustrates the colorimetric assay of the primary molecules involved in the synthesis and fate of acetyl-CoA. The pyruvate level in the H1975R+was approximately 10% higher ($p=0.002$), whereas that in the H1975R− was 9% lower ($p=0.01$) than that in the H1975P cells. Moreover, there was a 19% difference in pyruvate levels between the H1975R+and H1975R− cells ($p=0.0005$). The average level of acetyl-CoA in the H1975R+cells was 39% lower than that in H1975P, whereas the H1975R− cells exhibited an average increase of 14% in comparison to H1975P cells. However, this change was not statistically significant in either condition. Importantly, H1975R+cells displayed a significantly lower acetyl-CoA level (46%) than H1975R−cells ($P=0.02$). The concentration of ketone bodies was as follows: the level of acetoacetic acid (AcAc) was significantly elevated in the H1975R+cells, reaching trice that in H1975R− and H1975P cells ($p<0.0001$). Conversely, it was 14% lower in H1975R− cells than in H1975P cells ($p=0.02$). Alterations in β-hydroxybutyrate (BOHB) levels in the resistant cells relative to the parental cells were significant under both conditions. It increased by 40% in H1975R+cells ($p=0.02$) and decreased by 41% in H1975R− cells ($p=0.002$) compared to their respective H1975P cells. The H1975R+cells showed a 1.4-fold increase in BOHB levels relative to untreated cells ($p=0.002$). The H1975R+and H1975R− cells exhibited a reduction of 26% ($P=0.001$) and 5% ($P=>0.05$) in the levels of free fatty acids, respectively, in comparison to H1975P cells. Furthermore, the H1975R+cells displayed a 20% decrease in free fatty acid levels compared to H1975R− cells ($p=0.02$). The AcAc/BOHB ratio in H1975R+cells was 1.3-fold higher than that in H1975P cells. Conversely, H1975R-− cells exhibited a modest increase of 0.5-fold. The ratios of the H1975P, H1975R−, and H1975R+cells were 1.4, 2.1, and 3.2, respectively.

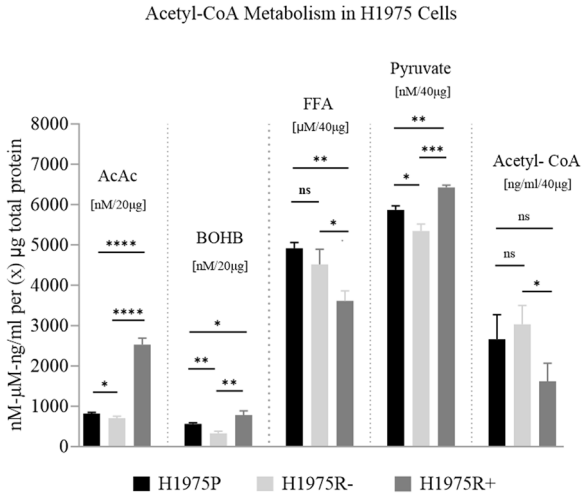

Fig. 4 Central carbon metabolism. Illustrates the comparison between acetyl-CoA and its primary precursors, namely pyruvate, free fatty acids (FFA), acetoacetic acid (AcAc), and 3-hydroxy butyrate (BOHB), in lung adenocarcinoma cells that are sensitive (H1975P) and resistant (H1975R) to Apitolisib. The levels of these substances per phenotype are measured per 20 μg of total cell protein. Additionally, the (R−) designation refers to H1975-resistant cells that are cultivated in Apitolisib-free medium (H1975R−), while H1975R+denotes resistant cells that are cultivated in medium containing 1 μM Apitolisib. (ns): $p=0.1–0.07$, (*): $p=0.01/0.02$, (**): $p=0.001–0.0009$, (***): $p<0.0001$

Drug combination: Fig. 5 illustrates the effect of Vorinostat, a pan-HDAC inhibitor, on the survival and proliferation rates of H1975P, H1975R+cells, and H1975R− cells. The H1975R− cells demonstrated a higher tolerance to a wide range of Vorinostat concentrations compared to H1975P and H1975R+cells. Unlike H1975R+and H1975P cells, the H1975R− cells did not show any response to Vorinostat at 4 μM final concentration (log doses of 3.6 nM). Pre-treatment with 1 μM Apitolisib (H1975R+), the survival rate of the resistant cells decreased by nine-fold when exposed to a dose of 7 μM Vorinostat (log dose 3.8 nM), reducing viability from 100% to only 10%. In contrast, when exposed to 7 μM (log dose of 3.8 nM), H1975R− cell survival only decreased by 20%. At a dose of 8 μM (log dosage of 3.9 nM), the viability of H1975R- cells were 57% compared to the control dosage, in which their viability remained unaffected. The viability of the H1975R+at this dose was only 5.5%, and when compared with the H1975R− cells, the H1975R+cells experienced a 9.5-fold greater reduction in viability. Dosages of 10 and 13 μM (log dosage 4.0 and 4.1 nM) did not have an additional cumulative effect on H1975R+cells, whereas their effect on H1975R− cells maintained a direct relationship, resulting in a reduction

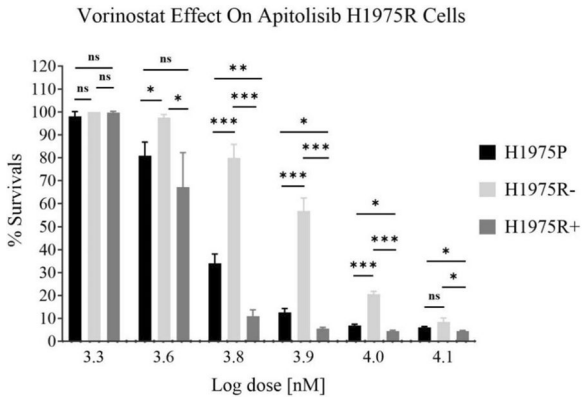

Fig. 5 The effect of Vorinostat on lung adenocarcinoma H1975 cells. The sensitive cells, which had not been exposed to Apitolisib (H1975P), were compared to both Apitolisib-resistant cells that had been incubated with Apitolisib (H1975R+) and those that had not been incubated with Apitolisib (H1975R−). Doses that were ≤ the logarithmic dose 2.1 nM did not have any significant effects on the three aforementioned phenotypes. (ns): $p = 0.1–0.3$, (*): $p = 0.001/0.0008$, (**): $p = 0.000001–0.000008$, (***): $p < 0.000001$

in their viability by factors of 2.6 and 5, respectively, compared to 8 μM (log dose 3.9 nM).

Discussion

The aim of this study was to examine the behaviour of Apitolisib-resistant H1975 lung adenocarcinoma cells from the perspective of metabolic reprogramming and proliferation aggressiveness. The notion was to shed light on how clinicians might proceed when malignant tissues have stopped responding to Apitolisib: continue or stop Apitolisib, or consider a drug combination. Therefore, understanding cancer biology and expanding the treatment team to include experts from different disciplines could improve patient outcomes. In our study, to model tyrosine kinase inhibitor resistance arising in the clinic, we used H1975 lung adenocarcinoma cells resistant to Apitolisib, and compared them to their parent sensitive cells.

Apitolisib reverted the excessive proliferation of resistant H1975R− cells

The confluency test and proliferation rate measurements showed that the H1975R− had an aggressive proliferation rate even higher than that of drug-naïve parent cells. However, the proliferation rate was suppressed by incubation with this drug (Fig. 1). Clinically, this means that stopping Apitolisib allows the tumour to become very aggressive, making tumour relapse highly probable. To elucidate the reasons for the relatively slow rate of proliferation observed in H1975R+ cells compared with H1975R− cells, we conducted cell cycle profiling. Interestingly, the cell cycle patterns in the treated and untreated cells were identical. However, the G0/G1 ratio of the newly dividing resistant cells was reduced by a factor of five compared to that of their parent cells. Moreover, the S and G2/M phases both doubled, indicating that both cell populations were actively dividing. The only discernible difference between the two cell populations was the energy output, which was scarce in the treated cells. To examine such hypothesis, seahorse energy phenotyping and central carbon metabolism assessment were performed (Figs. 3 and 4).

The inverted Warburg effect reflects the increased aggressiveness of H1975R− cells

An imbalance of the tyrosine kinase cascade can result in malignant transformation. This imbalance could be caused by gain-of-function (driver) mutations or increased expression of RTK or NRTK, combined with loss of apoptosis function, and in response to adaptive mitochondrial function. Consequently, in response to the increased demand for glucose for nucleic acid synthesis, somatic cells may activate alternative metabolic pathways to generate energy. This could involve an increased reliance on glycolysis, which accounts for up to 60% of cancer cell energy sources [14]. In cancer cells, the rate of glycolysis is 100× faster than that in normal somatic cells [15, 16], raising the amount and rate of glucose entry into the cells [7–9, 17–19]. The PI3K signalling pathway plays a role in regulating the cellular metabolism balance, between the aerobic and anaerobic pathways, and the uptake of glucose and other nutrients, as well as mitochondrial function [18, 19]. Inhibition of PI3K signalling by Apitolisib disrupts the balance between the dominant OXPHOS pathway and glycolysis, resulting in suppression of both pathways [20]. A large depression in energy production lowers the proliferation rate (Figs. 1 and 3). As a consequence of PI3K pathway inhibition, cancer cells begin to tolerate and adapt to several mechanisms to cope with this shift in energy. The ability of cancer cells to tolerate a one-log-fold increase in the IC50 of an inhibitor is called resistance. Apitolisib is a PI3K/m-TOR dual inhibitor was introduced in clinical trials after tumour cells become tolerant to PI3K single inhibitors. Resistance to this dual inhibitor has been well-documented in clinical trials to be due to either intrinsic genetic makeup or acquired resistance via exposure and adaptation [21].

H1975 cells harbour activated EGFR and a mutant PI3KCA enzyme downstream (a mutation in the catalytic subunit of the kinase enzyme) in combination with a dysfunctional TP53 gene. Their adaptive response to repetitive exposure to Apitolisib might involve activation of molecular crosstalk with EGFR, such as the EGFR/MAPK axis and other growth factor receptor signalling,

which can bypass the PI3K/m-TOR tyrosine kinases, activating the downstream transcription factors [21]. Therefore, these cells can tolerate higher doses of Apitolisib over time and can sustain minimal energy requirements. Our findings show that when Apitolisib-resistant cells are incubated with the drug, the inhibition of PI3K may disrupt metabolic regulation, leading to a shift towards non-glucose substrate aerobic metabolism, which is confirmed by their increased consumption of fatty acids, accumulation of pyruvate and elevated levels of ketone bodies (ketosis), combined with their decreased OCR and ECAR (Figs. 3 and 4) [22]. This could be attributed to Apitolisib, as a PI3K inhibitor, leading to additive suppression of both mitochondrial OXPHOS and glycolysis, as well as to the reduction of glucose uptake by GLUT transporters, which would limit the availability of glucose for metabolic processes and nucleic acid synthesis [10, 23].

In Apitolisib-free media, resistant cells (H1975R) shifted to an aerobic metabolism phenotype (a reversed Warburg effect) driven by energy starvation caused by Apitolisib. These cells became more energetic than their parent cells, as indicated by their increased OCR, increased pyruvate consumption, and lowered ketone body levels (Figs. 3 and 4). These highly energetic cells point to the restoration of PI3K/mTOR- facilitated glucose influx and its utilization via mitochondria, with glucose scarcity caused by Apitolisib acting as a driving force (Fig. 3), as well as extra energy sourced through non-carbohydrate substrates (reversed Warburg effect). This explains why Apitolisib-resistant H1975 cells in drug-free medium exhibit high proliferation rates.

Elevation of ketone bodies explains the slow proliferation rate of treated H1975R+ cells

Accumulation of ketone bodies and increased consumption of fatty acids can slow cancer cell proliferation and invasion, which is the case in H1975R+ cells [24]. The opposite pattern was observed in non-treated cells, in which the diminished levels of ketone bodies reflected the adequacy of their glucose supply for a high proliferation rate (Fig. 1). Ketone bodies have been shown to inhibit the proliferation of cancer cells and induce apoptosis, leading to reduced tumour growth. They can also diminish glycolytic flux and glutamine uptake in tumour cells, resulting in decreased ATP content and survival [25]. Increased ketone bodies in resistant cancer cells disrupt their survival and proliferation, inhibit glycolysis, and block the main pathway of energy production [24, 26]. Ketone supplementation or a ketogenic diet has shown positive therapeutic advantages in various malignancies, potentially targeting tumour metabolism as a new area for drug discovery [27]. The molecular pathways affected by ketone body treatment in cancer cells include the JAK-STAT and mTOR pathways, which lead to decreased cell migration and inhibition of cellular growth and proliferation. This might explain the activated JAK/STAT axis in our treated Apitolisib-resistant H1975 cells published earlier by the thoracic oncology research group at TTMI, Trinity College, Dublin [28]. The acquired reliance on the JAK-STAT signalling pathway might make them less vulnerable to the inhibitory effect of Apitolisib. In the absence of the drug, these cells can still exploit alternative PI3K-independent growth promoting pathways to achieve a higher proliferation rate.

Apitolisib-resistant H1975R− cells tolerate higher doses of vorinostat than H1975R+

HDACs play a vital role in the transcription of genes involved in cell cycle progression and survival. Furthermore, HDACs 1–7 are essential for the transcription complexes required for the cell cycle and survival [29]. HDAC7 has been found to be a significant contributor to cancer cell proliferation because it affects cell cycle progression by regulating c-Myc expression [30]. Thoracic oncology research group at TMMI-TCD reported that Apitolisib activates c-Myc expression in Apitolisib-treated resistant H1975 cells [31], which was also the subject of the current study. It has been demonstrated that HDAC inhibitors impede proliferation and induce apoptosis in tumour cells, indicating that they may affect the post-translational modifications of molecules involved in cell proliferation and survival [31, 32]. Western blot analysis of HDAC levels in H1975R+ cells revealed elevated levels of HDACs 1, 2, 3, 4, and 6 compared with H1975R− cells (H1975R−) [13]. When a pan-HDAC inhibitor was employed, the H1975R− cells demonstrated tolerance to elevated doses of Vorinostat, whereas the H1975R+ cells exhibited significant vulnerability to Vorinostat (Fig. 5). This observation contradicts the findings from the western blot analysis, which suggests that the H1975R+ cells should have a higher tolerance to Vorinostat because of their elevated levels of HDACs compared to the non-treated cells (H1975R−) [13]. However, this elevation in HDACs may indicate inactivity, and a positive feedback mechanism may trigger their expression and promote protein abundance. The PI3K/mTOR pathway is known to induce phosphorylation of HDACs, thereby preventing their export to the nucleus and serving as transcriptional corepressors. We anticipated that treatment with Apitolisib would result in hypo-phosphorylation of HDACs. This hypo-phosphorylation of HDAC IV and V in H1975R+ cells was opposite to that in H1975R− cells, which indicates that these HDACs are inactive [13]. This finding indicates that HDACs play a significant role in the resistance of.

H1975 cells to Apitolisib and that their phosphorylation is essential for their functionality. As HDACs become more phosphorylated, their proliferation rates increase, and vice versa. This interpretation is supported by the higher proliferation rate observed in the H1975R− cells (Fig. 1).

In summary, Apitolisib reduced the survival of H1975R+ with exceedingly low levels of energy, resulting in a significant reduction in their proliferation rate (Fig. 1). This phenomenon may be attributed to a higher rate of apoptosis in comparison to the newly generated cells, which is caused by the compromise of both mitochondria and glycolysis by Apitolisib. This is indicated by heightened levels of ketone bodies and increased consumption of fatty acids. Additionally, Apitolisib has been observed to eliminate the phosphorylation of HDACs, thereby facilitating their entry into the nucleus to function as a co-repressor of genes essential for cell survival and proliferation. Upon discontinuation of Apitolisib, the phosphorylation of HDACs was restored and their expression diminished. This suggested the increased abundance of HDACs might stem from a feedback mechanism. Inhibitors of HDACs impede proliferation and induce apoptosis in tumour cells, indicating that they might affect post-translational modifications of molecules involved in cell proliferation and survival. Additionally, by interacting with checkpoint kinases and reducing the expression of cyclin-dependent kinase inhibitory genes, such as BAX and P21, which promote apoptosis through the activation of P53, these inhibitors further contribute to the higher proliferation of non-treated H1975 resistant cells. This finding was supported by western blot analysis [13]. Considering this scenario in the context of the in vivo resistance to Apitolisib observed in clinical settings, it can be inferred that if the medication is stopped, the elevated levels of HDACs become vulnerable to PI3K/AKT, resulting in a significant increase in phosphorylated HDACs, ultimately facilitating tumour relapse and enhancing aggressiveness. Therefore, it is highly recommended not to stop Apitolisib when no further clinical improvement obtained, and instead to combine with HDAC inhibitors. However, one limitation of this study is that we need to bear in mind that the specific effects of Apitolisib on cellular metabolism and the cell cycle may depend on several factors, such as cell type, genetic alterations, and the cell's microenvironment. Therefore, further investigation of the metabolic effects of Apitolisib on resistant cells within panels of cell lines with varying oncogenicities would yield more comprehensive insights into these processes. The other limitation is that even with the use of a panel of cell lines, tumour tissues are highly heterogeneous and culturing cell suspension of patients' tissues is not being used for testing drugs in translational medicine laboratories.

Conclusions

Due to high levels of cross-talk signalling activation of tyrosine kinases, adaptation to their inhibitors is inevitable, and as highlighted in the limitation of this study, resistance to this type of targeted chemotherapy might come from alteration in the genetic makeup of malignant tissues and their heterogeneity. Therefore, when the tumour starts to grow slowly and the resistance to Apitolisib is highly likely, it is strongly recommended to continue the drug and combine it with the available, proven, effective drug combination. Additionally, expanding the role of translational research laboratories in hospitals would have a substantial positive impact on the overall patient outcome.

Abbreviations

ACAC	Acetoacetic acid
ATP	Adenosine triphosphate
BAX	BCL2-associated X factor apoptosis regulator
BOHB	Beta hydroxyl butyrate
DAPI	4′, 6-Diamidino-2-phenylindole
ECAR	Extra cellular acidification rate
EGFR	Epidermal growth factor receptor
ELISA	Enzyme-linked immunosorbent assay
FBS	Foetal bovine serum
FDA	Food and drug administration
FFA	Free fatty acids
GLUT	Glucose transporters
H1975P	Lung adenocarcinoma cell line haven't been exposed to Apitolisib or any other treatment
H1975R−	Lung adenocarcinoma cell line passaged in Apitolisib-free RPMI media
H1975R+	Lung adenocarcinoma cell line passaged in RPMI 1 μM Apitolisib (final concentration) containing media
HDAC	Histone deacetylase
HDACi	HDAC inhibitor
Jak	Janus kinase
MAPK	Mitogen-activated protein kinase
NRTK	Non-receptor tyrosine kinases
OCR	Oxygen consumption rate
OD	Optical density
OXPHOS	Oxidative phosphorylation
PPR	Proton production rate
PBS	Phosphate-buffered saline
PI3K	Phosphoinositide 3-kinase
PI3KCA	Phosphoinositide 3-kinase catalytic subunit
RPMI	Rosewell park memorial institute
RT	Room temperature
RTK	Receptor tyrosine kinases
PI3K/mTOR	Phosphoinositide 3-kinase/Mammalian target of rapamycin
STAT	Signal transducer and activator of transcription
TCD	Trinity College Dublin
TK	Tyrosine kinase
TKI	Tyrosine kinase inhibitors
TTMI	Trinity translational medicine institute

Acknowledgements

We would like to acknowledge Dr. Kathy Gately for gifting us the cell lines, and for her exceptional advice and assistance at Trinity Translational Medicine Institute (TTMI) at Saint James's Hospital, Trinity College Dublin. Furthermore, we acknowledge Dr. Jacintha O'Sullivan from TTMI for her invaluable assistance on metabolic profiling and seahorse training. We also extend our thanks to

Dr. Mary O'Sullivan, Dr. Sharon O'Toole and Dr. Bashir Mohamed from TTMI for the training and the use of the Cytell® machine for cell cycle analysis. Special thanks also extended to Prof. Dr. Paul Moynagh and the administrative staff at the department of biology, faculty of engineering and biomedical sciences -Maynooth University for their effective communication in facilitating our research. N.B: This research work has not been published as a paper prior to date. This work has been submitted to Cureus journal couple of weeks ago but withdrawn because the length of the manuscript gone beyond the free APC.

Author contributions
Abduladim Hmmier contributed to the design of the study, conducted all the research experiments, result analysis and to writing of the manuscript. Paul Dowling contributed to the design of the study, revised the manuscript, and supervised all research experiments.

Funding
This research work was funded by a scholarship from the Ministry of Higher Education and Scientific Research of Libya.

Availability of data and material
The datasets used and/or analysed during the current study are available from the corresponding author on reasonable request.

Declarations

Ethics approval and consent to participate
Not applicable.

Consent for publication
This research work is part of the corresponding author PhD research work and agreed between me and my supervisor to publish.

Competing interests
None of the authors has a conflict of interest to disclose.

Received: 22 May 2024 Accepted: 19 September 2024
Published online: 27 September 2024

References

1. Akekawatchai C, Jitrapakdee S (2023) Cellular signals integrate cell cycle and metabolic control in cancer. Adv Protein Chem Struct Biol 135:397–423. https://doi.org/10.1016/bs.apcsb.2023.01.002
2. McDonell LM, Kernohan KD, Boycott KM, Sawyer SL (2015) Receptor tyrosine kinase mutations in developmental syndromes and cancer: two sides of the same coin. Hum Mol Genet 24(R1):R60–R66. https://doi.org/10.1093/hmg/ddv254
3. Huang L, Jiang S, Shi Y (2020) Tyrosine kinase inhibitors for solid tumors in the past 20 years (2001–2020). J Hematol Oncol 13(1):143. https://doi.org/10.1186/s13045-020-00977-0
4. Johnson M, Garassino MC, Mok T, Mitsudomi T (2022) Treatment strategies and outcomes for patients with EGFR-mutant non-small cell lung cancer resistant to EGFR tyrosine kinase inhibitors: focus on novel therapies. Lung Cancer 170:41–51. https://doi.org/10.1016/j.lungcan.2022.05.011
5. Yang Y, Li S, Wang Y, Zhao Y, Li Q (2022) Protein tyrosine kinase inhibitor resistance in malignant tumors: molecular mechanisms and future perspective. Signal Transduct Target Ther 7(1):329. https://doi.org/10.1038/s41392-022-01168-8
6. Morandi A, Taddei ML, Chiarugi P, Giannoni E (2017) Targeting the metabolic reprogramming that controls epithelial-to-mesenchymal transition in aggressive tumors. Front Oncol 7:40. https://doi.org/10.3389/fonc.2017.00040
7. Saikia S, Ahmed F, Prajapati BG, Vijaya Padma V, Chorawala RM, Postwala IH et al (2023) Reprogramming of lipid metabolism in cancer: new insight into pathogenesis and therapeutic strategies. Curr Pharm Biotechnol 24(15):1847–1858
8. Vettore L, Westbrook RL, Tennant DA (2020) New aspects of amino acid metabolism in cancer. Br J Cancer 122(2):150–156. https://doi.org/10.1038/s41416-019-0620-5
9. Schiliro C, Firestein BL (2021) Mechanisms of metabolic reprogramming in cancer cells supporting enhanced growth and proliferation. Cells. https://doi.org/10.3390/cells10051056
10 Alberghina L (2023) The Warburg effect explained: integration of enhanced glycolysis with heterogeneous mitochondria to promote cancer cell proliferation. Int J Mol Sci. https://doi.org/10.3390/ijms242115787
11 Ortiz-González A, González-Pérez PP, Cárdenas-García M, Hernández-Linares MG (2022) Prediction on the PI3K/AKT/mTOR Pathway of the antiproliferative effect of O. joconostle in breast cancer models. Cancer Inform. https://doi.org/10.1177/11769351221087028
12 Wright SCE, Vasilevski N, Serra V, Rodon J, Eichhorn PJA (2021) Mechanisms of resistance to PI3K inhibitors in cancer: adaptive responses, drug tolerance and cellular plasticity. Cancers (Basel). https://doi.org/10.3390/cancers13071538
13. Hmmier A (2018) Identification of lung carcinoma biomarkers associated with tumour development and drug resistance. National University of Ireland Maynooth, Maynooth
14 Jiang B (2017) Aerobic glycolysis and high level of lactate in cancer metabolism and microenvironment. Genes Dis 4(1):25–27. https://doi.org/10.1016/j.gendis.2017.02.003
15. Jin L, Zhou Y (2019) Crucial role of the pentose phosphate pathway in malignant tumors. Oncol Lett 17(5):4213–4221. https://doi.org/10.3892/ol.2019.10112
16 Zheng J (2012) Energy metabolism of cancer: glycolysis versus oxidative phosphorylation (review). Oncol Lett 4(6):1151–1157. https://doi.org/10.3892/ol.2012.928
17 Irshad R, Tabassum S, Husain M (2023) Aberrant lipid metabolism in cancer: current status and emerging therapeutic perspectives. Curr Top Med Chem. https://doi.org/10.2174/1568026623666230522103321
18 Tan J, Yu Q (2013) Molecular mechanisms of tumor resistance to PI3K-mTOR-targeted therapy. Chin J Cancer 32(7):376–379. https://doi.org/10.5732/cjc.012.10287
19. Hong SY, Yu FX, Luo Y, Hagen T (2016) Oncogenic activation of the PI3K/Akt pathway promotes cellular glucose uptake by downregulating the expression of thioredoxin-interacting protein. Cell Signal 28(5):377–383. https://doi.org/10.1016/j.cellsig.2016.01.011
20 Mishra R, Patel H, Alanazi S, Kilroy MK, Garrett JT (2021) PI3K inhibitors in cancer: clinical implications and adverse effects. Int J Mol Sci. https://doi.org/10.3390/ijms22073464
21 Yang J, Nie J, Ma X, Wei Y, Peng Y, Wei X (2019) Targeting PI3K in cancer: mechanisms and advances in clinical trials. Mol Cancer 18(1):26. https://doi.org/10.1186/s12943-019-0954-x
22. Kolb H, Kempf K, Röhling M, Lenzen-Schulte M, Schloot NC, Martin S (2021) Ketone bodies: from enemy to friend and guardian angel. BMC Med 19(1):313. https://doi.org/10.1186/s12916-021-02185-0
23. Dockx Y, Vangestel C, Van den Wyngaert T, Huizing M, De Bruycker S, Pauwels P et al (2021) Early changes in [18F] FDG uptake as a readout for PI3K/Akt/mTOR targeted drugs in HER-2-positive cancer xenografts. Mol Imaging 2021:5594514
24. Hwang CY, Choe W, Yoon KS, Ha J, Kim SS, Yeo EJ et al (2022) Molecular mechanisms for ketone body metabolism, signaling functions, and therapeutic potential in cancer. Nutrients. https://doi.org/10.3390/nu14224932
25 Feng S, Wang H, Liu J, Aa J, Zhou F, Wang G (2019) Multi-dimensional roles of ketone bodies in cancer biology: opportunities for cancer therapy. Pharmacol Res 150:104500. https://doi.org/10.1016/j.phrs.2019.104500
26. Miller AI, Diaz D, Lin B, Krzesaj PK, Ustoyev S, Shim A et al (2023) Ketone bodies induce unique inhibition of tumor cell proliferation and enhance the efficacy of anti-cancer agents. Biomedicines. https://doi.org/10.3390/biomedicines11092515
27 Saris CGJ, Timmers S (2022) Ketogenic diets and Ketone suplementation: a strategy for therapeutic intervention. Front Nutr 9:947567. https://doi.org/10.3389/fnut.2022.947567
28 Luszczak S, Kumar C, Sathyadevan VK, Simpson BS, Gately KA, Whitaker HC et al (2020) PIM kinase inhibition: co-targeted therapeutic approaches in prostate cancer. Signal Transduct Target Ther 5(1):7. https://doi.org/10.1038/s41392-020-0109-y

29 Citro S, Miccolo C, Meloni L, Chiocca S (2015) PI3K/mTOR mediate mitogen-dependent HDAC1 phosphorylation in breast cancer: a novel regulation of estrogen receptor expression. J Mol Cell Biol 7(2):132–142. https://doi.org/10.1093/jmcb/mjv021
30. Zhang Y, Ding P, Wang Y, Shao C, Guo K, Yang H et al (2023) HDAC7/c-Myc signaling pathway promotes the proliferation and metastasis of choroidal melanoma cells. Cell Death Dis 14(1):38. https://doi.org/10.1038/s41419-022-05522-0
31 Yuen HF, Gunasekharan VK, Chan KK, Zhang SD, Platt-Higgins A, Gately K et al (2013) RanGTPase: a candidate for Myc-mediated cancer progression. JNatl Cancer Inst 105(7):475–488. https://doi.org/10.1093/jnci/djt028
32. Gagliano T, Kerschbamer E, Baccarani U, Minisini M, Di Giorgio E, Dalla E et al (2024) Changes in chromatin accessibility and transcriptional landscape induced by HDAC inhibitors in TP53 mutated patient-derived colon cancer organoids. Biomed Pharmacother 173:116374. https://doi.org/10.1016/j.biopha.2024.116374

Publisher's Note